Guo *et al. Biology Direct* (2025) 20:26
https://doi.org/10.1186/s13062-025-00620-3

Biology Direct

RESEARCH Open Access

HOXB4/METTL7B cascade mediates malignant phenotypes of hepatocellular carcinoma through TKT m6A modification

Enshuang Guo[1,2*†], Lei Li[3†], Jiankun Yang[4†], Yongjian Zhou[1,2], Lu Bai[1,2], Weiwei Zhu[1,2], Qiuyue Hu[1,2], Huifen Wang[1,2] and Hongqiang Liu[5]

Abstract

Background Hepatocellular carcinoma is a fatal malignancy that lacking specific therapies. Homeobox B4 (HOXB4) was negatively correlated with poor prognosis in cancers, but its role in hepatocellular carcinoma has not been elucidated.

Results We confirmed that HOXB4 was downregulated in hepatocellular carcinoma tissues and lower HOXB4 expression associated with poor prognosis. Gain- and loss-of function experiments were performed to understand the functional consequences. We revealed that HOXB4 overexpression inhibited proliferation and metastasis of hepatocellular carcinoma cells, accompanied with the decrease in epithelial-mesenchymal transition and increase in cell apoptosis. Database analysis showed that HOXB4 was positively correlated with the immune infiltration. PD-L1 expression was decreased in HOXB4 overexpressed hepatocellular carcinoma cells. HOXB4 overexpression was confirmed to inhibit the progression of hepatocellular carcinoma and promote T cell infiltration in vivo. N6-methyladenosine (m6A) modification was implicated in the tumorigenesis. RNA-seq analysis showed that HOXB4 overexpression modulated METTL7B expression. With the performance of dual-luciferase reporter, ChIP, and DNA pulldown assays, we revealed that HOXB4 binding to METTL7B promoter and inhibited its mRNA expression. The increased aggressiveness of hepatocellular carcinoma cells and the enhanced immune escape, triggered by HOXB4 knockdown, were inhibited via METTL7B downregulation. Methylated RNA immunoprecipitation assay displayed that METTL7B controlled the mRNA decay of TKT in m6A methylation. METTL7B overexpression increase the expression of TKT, ultimately promoting hepatocellular carcinoma progression and immune evasion.

Conclusions HOXB4 mediated the malignant phenotypes and modulated the immune evasion via METTL7B/TKT axis. The HOXB4/METTL7B cascade and its downstream changes might be novel targets for blocking hepatocellular carcinoma progression.

†Enshuang Guo, Lei Li and Jiankun Yang contributed equally to this work.

*Correspondence:
Enshuang Guo
fccguoes@zzu.edu.cn

Full list of author information is available at the end of the article

Graphical Abstract

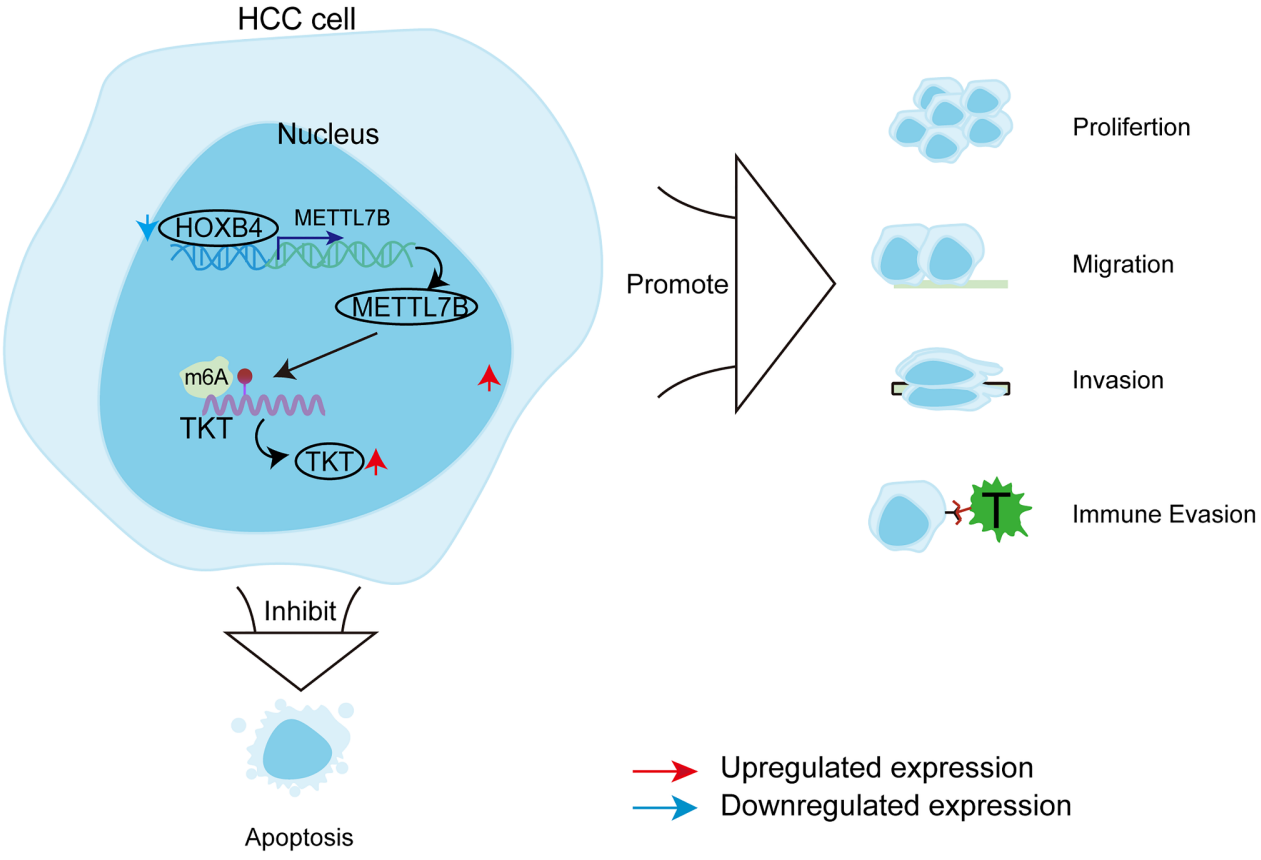

Keywords Hepatocellular carcinoma, Homeobox B4, Methyltransferase-like 7B, Malignant progression, Immune evasion

Introduction

Hepatocellular carcinoma (HCC) is a leading cause of cancer-related deaths worldwide [1, 2]. Although there have been significant advances in diagnostics, surgical techniques, targeted therapies, and immunotherapies, HCC remained a major public health concern. The 5-year overall survival rate of patients with HCC remained unsatisfactory due to the recurrence with distant metastasis and chemoresistance. Therefore, it is crucial to study target molecules and their molecular mechanisms in the development of HCC.

The abnormal expression of multiple genes and activation of signaling pathways has been demonstrated to participate in the development of HCC [3–5]. Homeobox (HOX) genes are a group of transcription factors that contain highly conserved homologous structural domains. It has been indicated that some HOX genes could serve as potential markers for HCC diagnosis and prognosis [6]. HOXD3 and HOXC10 have been shown to be involved in the progression of HCC [7, 8]. HOXB4 had effects in the malignant phenotypes of many tumors [9, 10], but its effects on HCC remain unknown. HOXB4 has been demonstrated to inhibit cervical cancer tumorigenesis by inhibiting cell proliferation [10]. The proliferation and migration of adult neural tube tumor and breast cancer were suppressed through HOXB4 overexpression [11, 12]. Immune infiltration is closely associated with the occurrence, development, and metastasis of tumors [13]. The expression level of HOXB4 had an apparently positive correlation with the presence of infiltrating immune cells in colon adenocarcinoma [9]. PD-L1 upregulation led to immune evasion of HCC cells [14], and HOXB4 might affect PD-L1 expression [15].

Abundant evidence has shown that epigenetic dysregulation contributes significantly to the development of HCC [16]. Nowadays, RNA methylation has attracted increasing attention. Among them, N6-methyladenosine (m6A) modification is the most predominant type of mRNA methylation in mammals [17]. m6A modification has been implicated in diverse biological processes

including tumorigenesis [18]. The effects of m6A were achieved through the dynamic interaction of methyltransferases, demethylases, and effector proteins. Several methyltransferase genes have been validated to be involved in the progression of HCC. METTL3 could promote HCC progression by enhancing m6A modification [19]. METTL18 was associated with immune infiltrates in HCC [20]. In the study of Ma et al., the metastatic ability of HCC cells could be suppressed by METTL14 [21]. The influence of other members of METTL family genes in the progression of HCC has not been studied. Therefore, we hypothesized that HOXB4 might affect the progression of HCC through influencing the expression of methyltransferase family genes. Transketolase (TKT) is an enzyme that presents in most tumor tissues. In HCC, TKT could promote cell proliferation, cell cycle, and migration [22]. The downregulation of TKT induced HCC cells apoptosis [23]. TKT activation could lead to immune escape and metastasis of HCC cells by increasing the expression of PD-L1 [24].

Based on this information, and using several in vitro and in vivo experiments, we aimed to explore the functional role of HOXB4 and the potential utility of its genetic modulation in hepatocarcinogenesis. Our observations characterized HOXB4 as a promising biomarker in HCC.

Materials and methods

Cell culture and treatment

HCC cell lines (Li-7, PLC/PRF/5, and Hepa1-6) were purchased from iCell Bioscience Inc (China). Normal hepatocyte cell line (THLE-2) was purchased from Procell Bioscience Inc (China). Li-7 cells were cultured in RPMI-1640 medium (Beijing Solarbio Science and Technology Co., Ltd, China) containing 10% fetal bovine serum (FBS, Zhejiang Tianhang Biotechnology Co., Ltd., China). PLC/PRF/5 cells were cultured in MEM medium (Solarbio) containing 10% FBS (Tianhang). THLE-2 cells were cultured in special medium (Procell). Hepa1-6 cells were cultured in DMEM medium (Servicebio Technology Co., Ltd., China) containing 10% FBS (Tianhang).

siRNAs targeting METTL7B and TKT were designed and transfected using Lipofectamine™ 3000 Transfection Reagent (Invitrogen, USA). The coding sequence of METTL7B was cloned into the pcDNA3.1 vector, and the plasmid was transfected using Lipo3000. Small hairpin RNA (shRNA) targeting HOXB4 was designed and cloned into the Tet-pLKO-Puro vector plasmid. The coding sequence of HOXB4 was cloned into the pLVX-TetOne-Puro vector plasmid. The appropriate concentration of lentivirus suspension was added to the cells. The stable cells were constructed using puromycin. To induce HOXB4 knockdown or overexpression, 1 μg/ml doxycycline (dox) was added to the dox + groups.

Methyl Thiazolyl tetrazolium (MTT) assay

MTT and dimethyl sulfoxide were purchased from Nanjing KEYGEN Biotech. Co., Ltd. (China). Five thousand cells were placed in 96-well plates, cultured for a certain time, and incubated with 50 μL MTT solution at 37 °C for 4 h. After removing the supernatant, dimethyl sulfoxide was added to each well. A microplate reader was used to measure the optical density at 490 nm.

TUNEL assay

TUNEL staining was performed to assess cell apoptosis using the In Situ Cell Death Detection Kit (Roche Diagnostics, Switzerland) following the manufacturer's instructions. The paraffin-embedded sections from were cut into 5 μm sections. The sections were then deparaffinized and hydrated. Sections were permeabilized using Triton X-100 and stained with TUNEL solution for 60 min at 37℃ in darkness. The antifading mounting medium was added after staining of the nuclei with DAPI for 5 min, and the results were visualized using a microscope.

Clone formation assay

The treated Li-7 and PLC/PRF/5 cells were placed in dishes (300 cells per dish) and incubated at 37 °C with 5% CO_2 for 14 days. Giemsa Stain Kit was purchased from Nanjing Jiancheng Biological Engineering Research Institute (China). Cells were fixed with R1 solution (from the kit) for 1 min followed by staining with R2 solution (from the kit) for 5 min. The clone formation rate was calculated after photographing.

Wound healing assay

Prior to the experiment, the medium was changed to serum-free medium and treated with mitomycin C (Sigma-Aldrich, USA) for 1 h. Constant-diameter strips were scratched with a 200 μL sterile Eppendorf pipette tip. Scratch widths at the same locations were measured after cultured for 0 h and 24 h.

Immunofluorescence

The coverslips were fixed with paraformaldehyde, permeabilized with Triton X-100, and blocked with 1% bovine serum albumin. The coverslips were incubated with E-cadherin antibody (#AF0131, Affinity, China), followed by incubating with anti-rabbit IgG (H + L, Alexa Fluor® 555 Conjugate) antibody (#4413, Cell Signaling Technology, USA). The coverslips were observed under a fluorescence microscope.

Flow cytometry analysis

Annexin V and PI staining were performed to determine the cell apoptosis with the Annexin V-FITC/PI Apoptosis Detection Kit (KEYGEN). The percentage of CD4 + T

cells and CD8 + T cells in the tumor tissues of mice was detected using flow cytometry. The detected cells were stained with CD4 (#FITC-65104) or CD8a (#FITC-65069) antibody at 4℃ for 30 min in the dark. CD4 and CD8a antibodies were purchased from Proteintech.

Real-time PCR (qPCR)

TRIpure reagent (BioTeke, China) was used to extract total RNA. BeyoRT™ II M-MLV reverse transcriptase (Beyotime Biotech Co., Ltd., China) was used to obtain the corresponding cDNA. qPCR was carried out with SYBR green (Solarbio) and 2×Taq PCR MasterMix (Solarbio). The relative expressions were calculated using the $2^{-\Delta\Delta}$CT method.

Western blotting

Tissues and cells were lysed in cell lysis buffer for Western and IP (Beyotime) with 1% phenylmethanesulfonylfluoride (PMSF). Extracted proteins were separated using Sodium dodecyl sulfate polyacrylamide gel electrophoresis and transferred onto polyvinylidene fluoride membranes. After being blocked with blocking buffer, the membranes were incubated with the primary antibody at 4 °C overnight. Western washing buffer (Beyotime) was used to wash the membranes. Subsequently, the membranes were incubated with secondary antibodies for 45 min at 37℃. Finally, the blots were detected with ECL chemiluminescence kit purchased from Beyotime. Ki67 (#AF0198), PCNA (#AF0239), Bax (#AF0120), Bcl-2 (#AF6139), cleaved caspase-3 (#AF7022), cleaved caspase-9 (#AF5244), active MMP-2 (#AF5330), active MMP-9 (#AF5228), E-cadherin (#AF0131), N-cadherin (#AF5239), Vimentin (#AF7013), and TKT (#DF13956) antibody were purchased from Affinity (China). HOXB4 (#A19699), METTL7B (#A7200), and PD-L1 (#A1645) antibody was purchased from ABclonal Technology Co., Ltd. (China).

Transwell assay

The invasive ability of cells was detected using Transwell chambers (Labselect, China). For invasion assays, the small chambers were coated with pre-diluted Matrigel (Corning, USA), and incubated at 37 °C for 2 h. Li-7 and PLC/PRF/5 cells were seeded in the upper chambers (8×10^4 cells per well), and 800 μL of cell culture medium containing 10% FBS was added to the bottom chambers. After being incubated for 24 h, the invasive cells were stained with 0.5% crystal violet staining solution (Amresco, USA) after being fixed with 4% paraformaldehyde for 20 min.

Dual-luciferase assay

Cells were co-transfected with the firefly luciferase plasmid (pGL3-basic, pGL3-METTL7B promoter (-2000 - +35), or pGL3-METTL7B promoter (-1500 - +35)) and HOXB4 expression plasmid (EV or HOXB4). The luciferase dual assay kit was purchased from KEYGEN and the dual luciferase activity assay was performed according to the manufacturer's instructions.

ChIP assay

After cross-linking with 1% formaldehyde and stopping with glycine solution, the cells were resuspended and sonicated. Chromatin extracts were immunoprecipitated with protein A + G Agarose/Salmon Sperm DNA from ChIP Assay Kit (Beyotime). After washing, elution, and de-crosslinking, the immunoprecipitated DNA was amplified and detected using agarose gel electrophoresis.

Pull-down assay

DNA pulldown kit was purchased from Bersinbio (China, #Bes5004). Protein was extracted using buffer 1 (from the kit) containing protease inhibitor and DTT. The probes were mixed with streptavidin agarose beads in DNA beads buffer for 30 min at 25℃. The cell lysates were incubated with the mixture of buffer and the probe-magnetic beads at 4 °C for 1 h. The bound proteins were identified via Western blotting after purification.

Animal experiment

All animal experiments were conducted in accordance with the ethical standards of animal care and approved by the Life Science Ethics Review Committee of Zhengzhou University (March 18, 2022). For tumor growth experiments, Li-7 or PLC/PRF/5 cells (5×10^6 cells per mouse) with HOXB4 overexpression or knockdown were subcutaneously injected into the BALB/c nude mice (6 weeks old). Mice were fed with water containing 10% sucrose and dox (2 mg/mL) after the tumors were visible. The volume of tumors was measured each 4 days. The mice were sacrificed on day 28, and the xenografted tumors were collected for further analysis. For studies on immune infiltration, Hepa1-6 cells (5×10^6 cells per mouse) with HOXB4 overexpression or knockdown were subcutaneously injected into the male C57BL/6 mice (6 weeks old). Mice were fed with water containing 10% sucrose and dox (2 mg/mL) after the tumors were visible. The volume of the tumor tissue was measured each 4 days. The mice were sacrificed on day 28, and the xenografted tumors were collected. Part of the tumor samples was removed, fixed, embedded in paraffin, and sectioned for hematoxylin and eosin staining.

Immunohistochemistry

The paraffin-embedded sections of xenografted tumor from mice were cut into 5 μm sections. The sections were deparaffinized, hydrated, and heated for 10 min in sodium citrate buffer for antigen retrieval. After being incubated with 3% H_2O_2 for 15 min to block endogenous

peroxidase, the sections were incubated with bovine serum albumin. The sections were then incubated with Ki-67 antibody or CD3 antibody at 4 °C overnight followed by incubating with secondary HRP-conjugated goat anti-Rabbit IgG for 60 min. After being incubated with 100 μL DAB solution, the sections were stained with hematoxylin for 3 min. The neutral resin was added to seal the sections after dehydration and transparency. The sections were visualized under a fluorescence microscope. The Ki-67 (#AF0198) and CD3 (#DF6594) antibody were purchased from Affinity.

RNA-seq

Total RNA was extracted, and the library was constructed, and RNA-seq was performed using Illumina. The criteria for differentially expressed genes were set up with an adjusted. p value (adj. p) < 0.005 and|log2Fold Change (Log2FC)| > 1.

Methylated RNA Immunoprecipitation

Methylated RNA immunoprecipitation was detected using riboMeRIPTM m6A Transcriptome Profiling Kit (Guangzhou Ribobio Co., LTD, China) in accordance with manufacturer's instructions. In short, 18 μg total RNA extracted from METTL7B-overexpressed Li-7 cells or its vector cells was isolated and randomly fragmented. One-tenth of fragmented RNA was saved as input. The fragmented RNA was then incubated with the IgG or m6A antibody in the immunoprecipitation buffer, which contained RNase inhibitor. The m6A-precipitated RNA was eluted the mixture of nuclease-free water, RNase inhibitor, 5 × IP Buffer, and N6-Methyladenosine. Modification of m6A was determined by qPCR analysis with specific primers.

Data source

We used the Kaplan-Meier plotter tool (http://kmplot.com/analysis/) to analyze the prognostic relevance of HOXB4 with HCC. Based on the auto selected, patients with HCC were categorized into two different groups with low and high HOXB4 expression. Then, the probability of overall survival, progression free survival, and relapse free survival were accessed using the default settings. TNMplot (https://www.tnmplot.com/) was conducted in this study to analyze expression across tumor tissues relative to control samples. JASPAR (https://jaspar.genereg.net/) was used to predict the binding sites of HOXB4 to the promoter region of METTL7B. GSE142278 and GSE101728 were downloaded from NCBI Gene Expression Omnibus database.

Statistical analysis

All statistical analyses were performed using GraphPad Prism software and expressed as mean ± SD. Statistical significance was determined by one-way ANOVA test, two-way ANOVA, or t-test. Differences with $p < 0.05$ were considered significant.

Results

HOXB4 is lowly expressed in hepatocellular carcinoma and negatively associated with poor prognosis

An increasing body of evidence indicated that HOX genes played crucial roles in HCC and might serve as the potential marker for HCC diagnosis and prognosis [6]. To identify the possible HOX family genes that potentially derived the progression of HCC, we downloaded an HCC dataset (GSE101728) from NCBI Gene Expression Omnibus database. The differentially expressed genes were screened out using a cutoff value of|Log2FC| > 1 and adjusted p value (adj.p) < 0.05 (Fig. 1a). Compared with other HOX genes, HOXB4 was the most significant downregulated gene in tumor tissues (Fig. 1b-c). Additionally, the HOXB4 expression was associated with survival in the TCGA cohort. The patients with higher HOXB4 expression exhibited higher overall survival, progress free survival, and relapse free survival (Fig. 1d-f). The results of PCR and Western blot also showed that HOXB4 was highly expressed in HCC cell lines than normal hepatocyte cells (Fig. 1g). Above results implied that the dysregulation of HOXB4 might be involved in the progression of HCC.

HOXB4 overexpression reduced malignancy phenotype in hepatocellular carcinoma cell lines

To evaluate the functional roles of HOXB4 in HCC progression, stable HOXB4 knockdown cell lines and stable HOXB4 overexpressed PLC/PRF/5 and Li-7 cell lines was established. The mRNA and protein levels of HOXB4 was confirmed in each cell lines (Fig. S1a-b). HOXB4 overexpression significantly reduced cell proliferation at 24-, 48-, and 72 h in all cell lines tested (Fig. 2a-b). These results were in line with the reductions in the colony formation and Edu expression in HOXB4 overexpressed cells (Fig. 2c-f). The implication of HOXB4 in HCC cell proliferation was further corroborated by demonstrating a significant reduction in PCNA protein expression in response to HOXB4 overexpressed Li-7 and PLC/PRF/5 cell lines (Fig. 2e and f). In addition, we found that HOXB4 overexpression resulted in cell apoptosis (Fig. 2h and Fig. S2d), accompanied with a significant decrease in Bcl-2 expression and the increase in BAX, cleaved caspase 3, and cleaved caspase 9 protein levels (Fig. 2i and Fig. S2e).

The effects of altering the expression of HOXB4 on the metastatic and invasive potential of HCC cells was detected by Transwell and wound healing experiments. Compared to the control group, the metastases and invasiveness of HCC cells was significantly reduced after

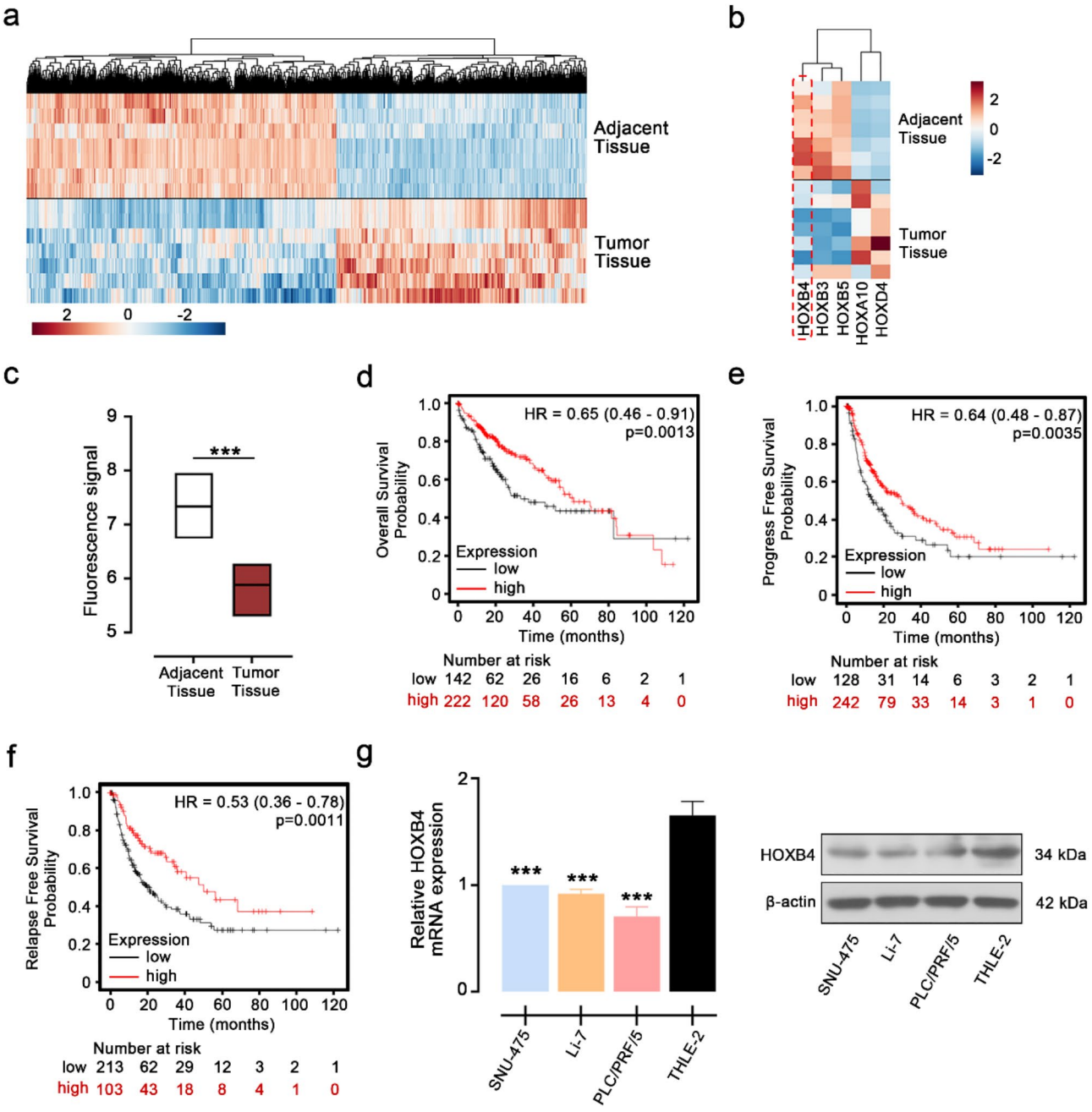

Fig. 1 HOXB4 is lowly expressed in hepatocellular carcinoma and negatively associated with poor prognosis. (**a**) Heatmap showing differential expression genes (DEGs) between adjacent normal tissues and HCC tissue samples. Data was obtained from NCBI Gene Expression Omnibus (GEO) (http://ncbi.nlm.nih.gov/GEO) with dataset accession number GSE 101,728.|Log2Fold Change (log2FC)| > 1 and adjusted *p* value (adj. *p*) < 0.05 were cutoff values; (**b**) Heatmap showing mRNA expression of homeobox family genes in GSE101728; (**c**) The expression of HOXB4 in HCC tissues and adjacent normal tissues from GSE101728, $^{***}p < 0.001$; (**d**-**f**) Kaplan-Meier analysis of overall survival (**d**), progress free survival (**e**), and relapse free survival (**f**) based on HOXB4 expression. (**g**) HOXB4 mRNA and protein expression and in hepatocellular cancer cell lines (SNU-475, Li-7, and PLC/PRF/5) and normal hepatocyte cell line (THLE-2). Data are expressed as mean ± SD, $N = 3$. $^{***}p < 0.001$

HOXB4 overexpression, whereas it was enhanced after HOXB4 knockdown (Fig. 3a-f). Several studies have reported that epithelial-mesenchymal transition (EMT) is the first step of HCC metastasis [25]. The increased expression of mesenchymal markers and concomitant loss of epithelial cell junction proteins induced the process of EMT [26]. Indeed, in vitro silencing of HOXB4 increased the protein expression of mesenchymal markers (active MMP-2, active MMP-9, N-cadherin, and Vimentin) and downregulated epithelial cell junction proteins (E-cadherin) protein levels in Li-7 and PLC/PRF/5 cells (Fig. 3g and Fig. S2a). The upregulation of

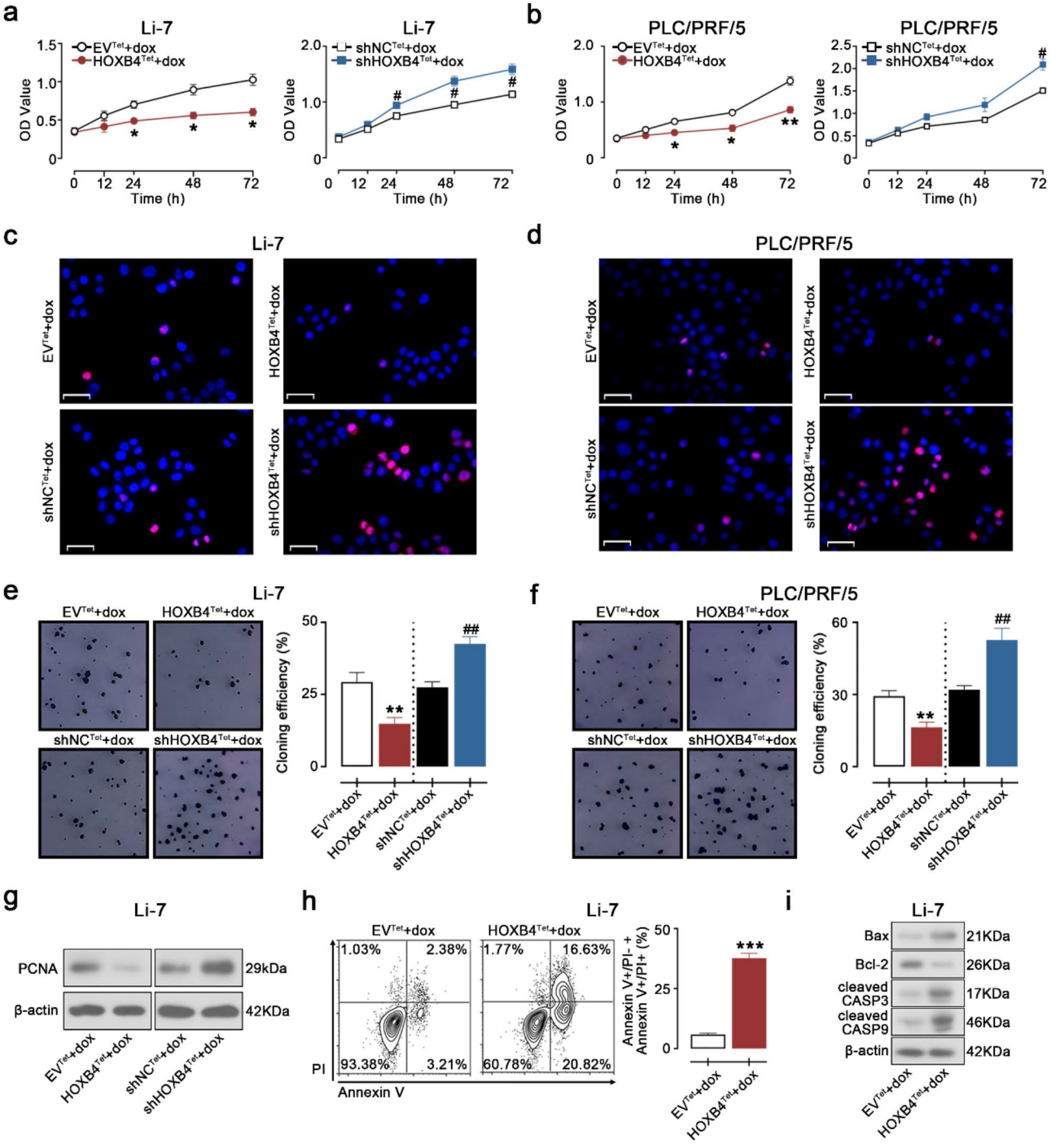

Fig. 2 HOXB4 inhibits proliferation and promotes apoptosis of hepatocellular carcinoma cell *in vitro*. (**a**-**b**) The proliferation of HCC cells with upregulated or downregulated HOXB4 expression; (**c**-**d**) EdU assay detected the proliferation of HCC cells with upregulated or downregulated HOXB4 expression. Scale bar, 50 μm; (**e**-**f**) Colony formation ability of HCC cells with upregulated or downregulated HOXB4 expression; (**g**) Representative immunoblots of PCNA in Li-7 cells with upregulated or downregulated HOXB4 expression; (**h**) Cell apoptosis of Li-7 cells with upregulated HOXB4 expression according to flow cytometry analysis; (**i**) Representative immunoblots of Bax, Bcl-2, cleaved caspase 3, and cleaved caspase 9 protein levels in Li-7 cells with upregulated HOXB4 expression. Data are expressed as mean ± SD, $N = 3$. $^{**}p < 0.01$, $^{***}p < 0.001$ vs. EV^{Tet}+dox; $^{\#}p < 0.05$, $^{\#\#}p < 0.01$ vs. shNC^{Tet}+dox

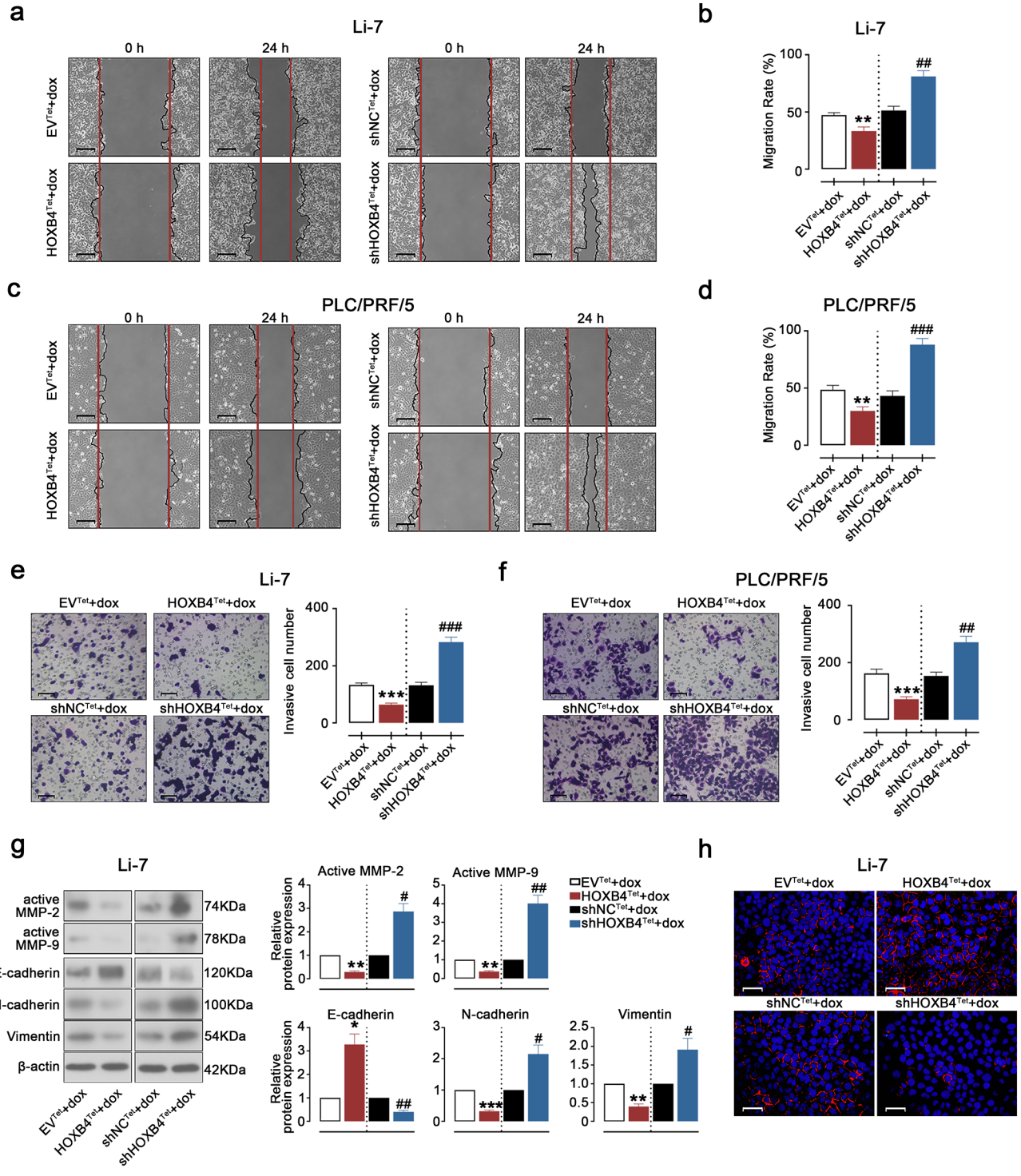

Fig. 3 HOXB4 suppresses migration and invasion via inhibiting EMT of hepatocellular carcinoma cell. (**a**-**d**) Representative images of wound healing experiments and quantitative data of migration of HCC cells with upregulated or downregulated HOXB4 expression. Scale bar, 200 μm; (**e**-**f**) Invasion ability of HCC cells with upregulated or downregulated HOXB4 expression was determined by Transwell assays. Scale bar, 100 μm; (**g**) Immunoblots analysis of active MMP-2, active MMP-9, E-cadherin, N-cadherin, and Vimentin in Li-7 cells with upregulated or downregulated HOXB4 expression; (**h**) Representative immunofluorescence images of E-cadherin expression in Li-7 cells with upregulated or downregulated HOXB4 expression. Scale bar, 50 μm. Data are expressed as mean ± SD, $N = 3$. $^{**}p < 0.01$, $^{***}p < 0.001$ vs. EV^{Tet}+dox; $^{\#}p < 0.05$, $^{\#\#}p < 0.01$, $^{\#\#\#}p < 0.001$ vs. shNC^{Tet}+dox

E-cadherin expression in HCC cells, triggered by HOXB4 overexpression, was also confirmed using IF staining (Fig. 3h and Fig. S2b). Taken together, HOXB4 overexpression might inhibit the migratory and invasive abilities of HCC cells by inhibiting EMT.

HOXB4 overexpression reduced the growth of xenografted hepatocellular carcinoma cell lines in nude mice

The effect of HOXB4 overexpression on HCC growth was evaluated in Li-7 and PLC/PRF/5-induced xenografts mouse model. HOXB4 overexpression significantly reduced tumor growth and the final tumor volume (Fig. 4a and d). Ki-67 staining reflect the effects

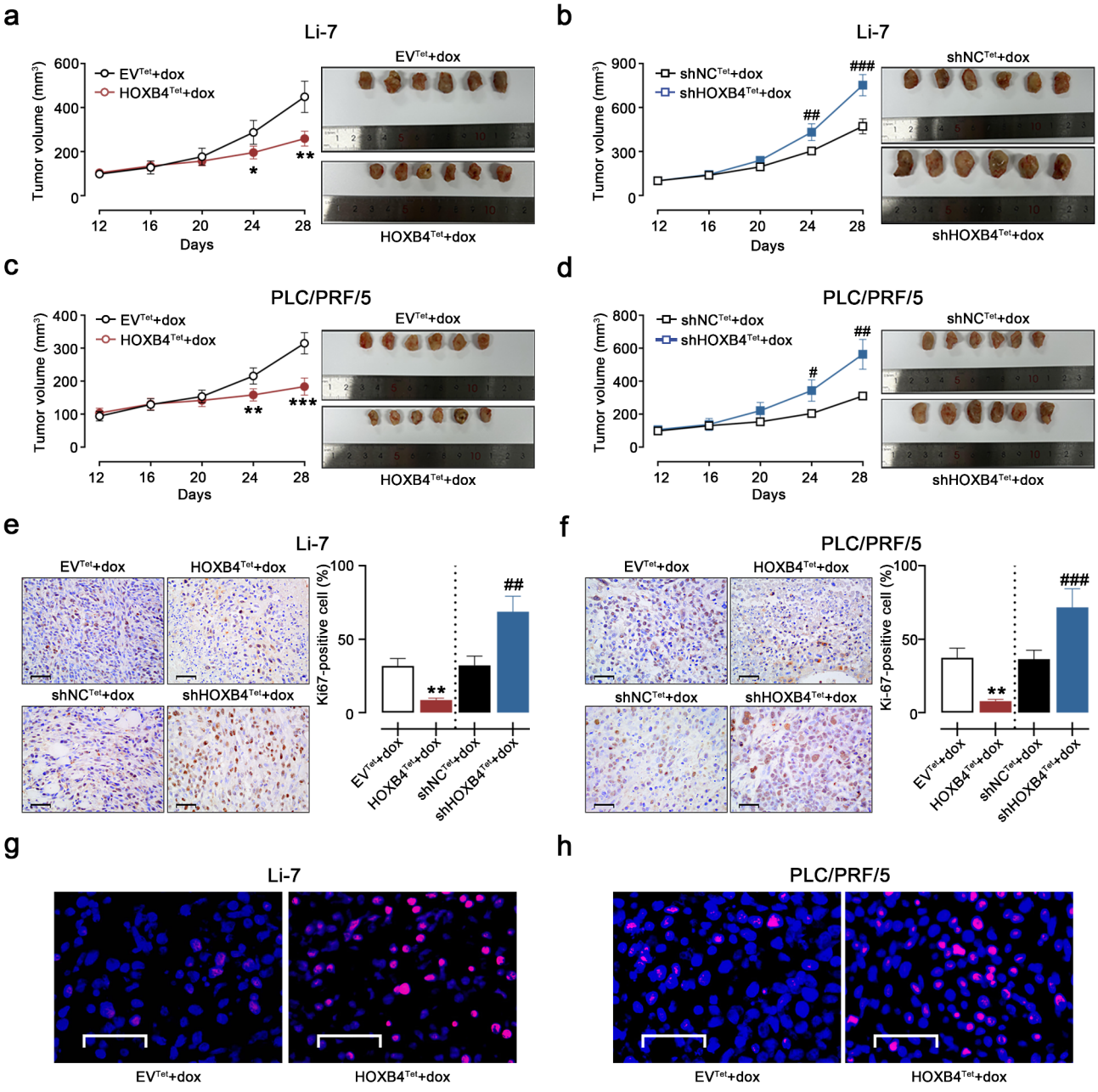

Fig. 4 Significant anti-tumor effects of HOXB4 overexpression in hepatocellular carcinoma *in vivo*. (**a**-**b**) Tumor volume and growth curves of subcutaneous xenogeneic tumor of BALB/c nude mice injected with indicated Li-7 cells, $N=6$; (**c**-**d**) Tumor volume and growth curves of subcutaneous xenogeneic tumor of BALB/c nude mice injected with indicated PLC/PRF/5 cells, $N=6$; (**e**-**f**) Immunohistochemical staining and quantitative data of Ki-67 in tumor tissues of BALB/c nude mice injected with HCC cells, $N=6$. Scale bar, 50 μm; (**g**-**h**) Representative TUNEL staining images of tumor tissues of BALB/c nude mice injected with HCC cells. Scale bar, 50 μm. Data are expressed as mean ± SD. $^{**}p<0.01$, $^{***}p<0.001$ vs. EV^{Tet}+dox; $^{\#}p<0.05$, $^{\#\#}p<0.01$, $^{\#\#\#}p<0.001$ vs. $shNC^{Tet}$+dox

of decreased cell proliferation in HOXB4 overexpression in vivo, and HOXB4 knockdown promoted Ki-67 expression in xenografted HCC tumor tissues (Fig. 4e and f). In addition, TUNEL labeling revealed that the HOXB4 overexpression group had a considerably higher apoptosis than the vector group (Fig. 4g and h). Collectively, our findings demonstrated that HOXB4 overexpression markedly inhibited HCC growth in vivo via decrease in tumor cell proliferation and increase in cell apoptosis.

HOXB4 overexpression promoted T-cell infiltration and inhibited immune evasion in hepatocellular carcinoma

Immune cell infiltration was highly associated with the initiation, development or metastasis of HCC [13], and HOXB4 expression could regulate the presence of infiltrating immune cells in colon adenocarcinoma [9]. Subsequent survival analysis found that the infiltration of CD8 + T cell and CD4 + T memory cell was positively associated with the survival rate of HCC, whereas neutrophil and M2 macrophage was negatively associated (Fig. 5a). Interestingly, HOXB4 expression was positively correlated with CD8 + T in HCC (Fig. 5b and c). We established stable HOXB4 knockdown cell lines and stable HOXB4 overexpressed Hepa1-6 cell lines to determine the direct role of HOXB4 in regulating T cells (Fig. 5d). The upregulation of Programmed cell death 1 ligand 1 (PD-L1) expression leads to an exhausted phenotype of CD8 + T cells and mediates tumor cell immune evasion [27, 28]. The HOXB4 overexpression inhibited the protein expression of PD-L1 in Hepa1-6 cells. C57BL/6 mice were subcutaneous inoculated with HOXB4-overexpressd and HOXB4-depleted cells. HOXB4 overexpression also contributed to decrease tumor growth in the immunocompetent mice (Fig. 5f and g). The immune infiltration was increase upon HOXB4 overexpression in tumor tissues (Fig. 5h). The effectiveness of HOXB4 knockdown and overexpression was validated at the protein levels (Fig. 5i). The protein expression of PD-L1 was also decreased in HOXB4 overexpression in vivo (Fig. 5i). We performed IHC analysis on tumor tissues, and HOXB4 overexpression enhanced CD3 + T-cell infiltration (Fig. 5j). Moreover, flow cytometry analysis confirmed that the proportion of CD8 + T and CD4 + T cells was elevated in HOXB4-overexpressed tumors (Fig. 5k, S3a-b). The aforementioned in vitro and in vivo results indicated that HOXB4 overexpression suppressed HCC progression through tumor immunity, which is correlated with infiltration and exhaustion of CD8 + T cells.

METTL7B is downregulated by HOXB4 and rescues the effects of HOXB4 in hepatocellular carcinoma cell

Our results showed that HOXB4 act as a tumor suppressor in HCC. Furthermore, we intended to determine its underlying mechanism in HCC cells. To predict the potential downstream factor of HOXB4, we performed RNA-seq using stable HOXB4-overexpressed and vector-transfected Li-7 cells. Principal component analysis showed the clear separation between HOXB4-overexpressed Li-7 cells and its vector cells (Fig. 6a). The heatmap was generated using a cutoff value of $|Log_2FC| > 1$ and adj. $p < 0.005$ (Fig. 6b). Epigenetic modifications have been implicated in the deregulation of HCC progression [29]. m6A methylation, a well-known modification with epigenetic functions, has been reported to participate in the tumorigenesis of HCC [30]. Methyltransferase (METTL) family genes were essential m6A writer [31], and several of its family genes were involved in the progression of HCC [32, 33]. RNA-seq data revealed that modulation of HOXB4 overexpression induced changes in a total of 18 m6A regulator genes. METTL7B was highly expressed in hepatic tissues, compared with other m6A regulated genes (Fig. 6c). Furthermore, METTL7B mRNA levels was significantly increased in HCC tissues (Fig. S4a). METTL7B was highly expressed in HCC cell lines (Fig. S4b). As shown in Fig. 6d, the mRNA expression of METTL7B was downregulated in HOXB4-overexpressed Li-7 cells. METTL7B has been shown to be associated with malignant phenotypes in many cancers [34–36]. Therefore, METTL7B attracted our attention as the downstream factor of HOXB4 because it has been poorly studied in HCC. PCR and Western blot analysis demonstrated that METTL7B expression was negatively regulated by HOXB4 in HCC cells (Fig. 6e and Fig. S4c), suggesting that HOXB4 might be a transcriptional repressor of METTL7B in HCC. We used JASPAR database predicted the possible binding region between HOXB4 and METTL7B, and ruled out one of the possibilities using the dual-luciferase reporter assay (Fig. 6f). The chromatin immunoprecipitation assay and pull-down assay showed that HOXB4 was recruited to the site (Fig. 6g and i). We detected the malignant phenotypes in Li-7 cells with METTL7B overexpression or knockdown (Fig. S4d), confirming that METTL7B overexpression promoted the malignant phenotypes of HCC (Fig. S4e-g). We downregulated METTL7B expression in HOXB4-depelted cells (Fig. 6j). The promotion of HCC cell activity, invasive, and immune evasion induced by HOXB4 downregulation was inhibited by METTL7B knockdown (Fig. 6k and m). Collectively, these results indicated that the anti-tumor effects of HOXB4 overexpression might achieve by transcriptionally inhibiting the METTL7B.

METTL7B altered TKT m6A modification and modulated the malignant phenotypes in hepatocellular carcinoma

METTL7B functions as an m6A writer, affecting translation of m6A-modified mRNA. To further identify

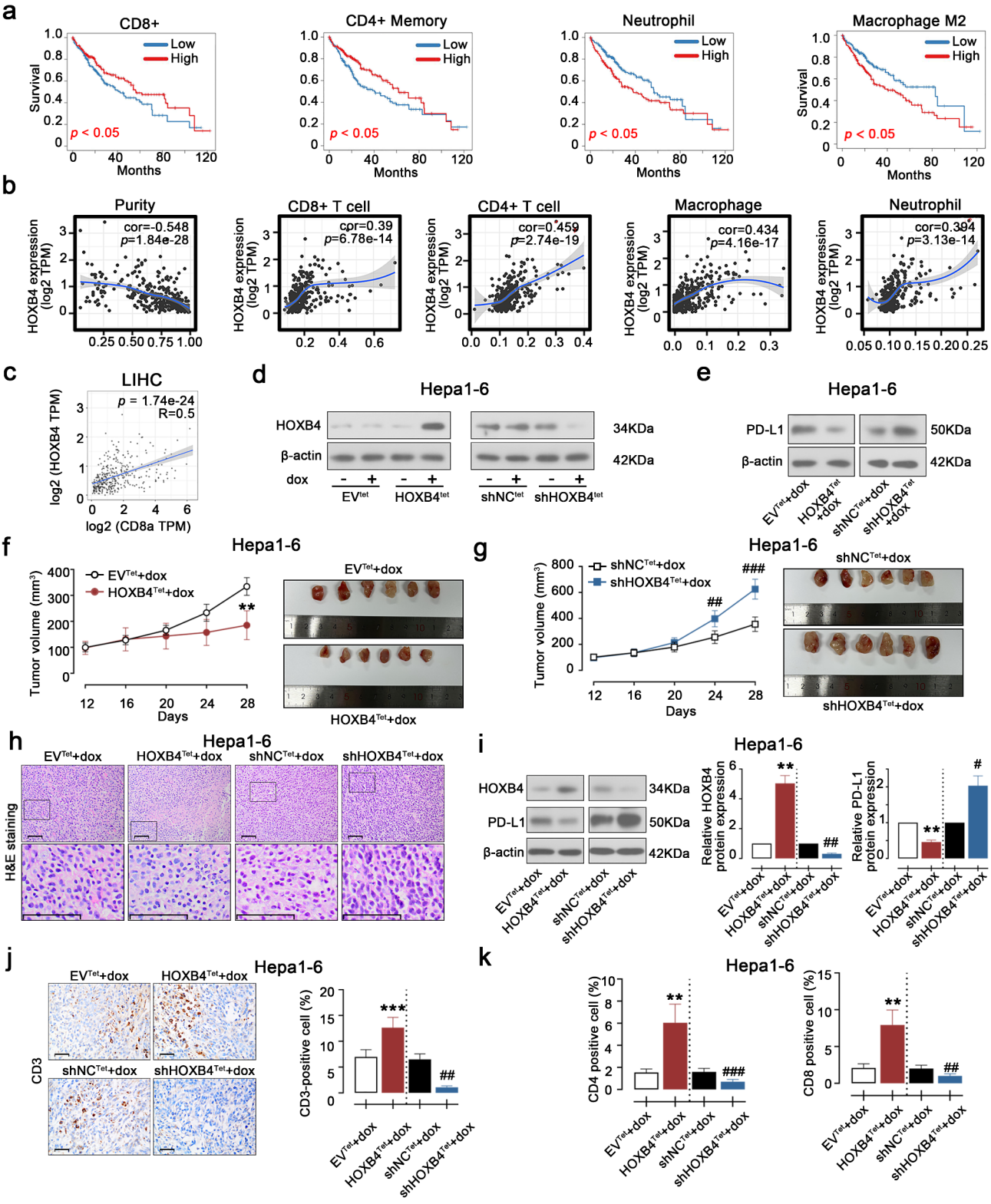

Fig. 5 (See legend on next page.)

(See figure on previous page.)

Fig. 5 HOXB4 suppresses PD-L1 expression and promotes tumor immune infiltration in hepatocellular carcinoma. (**a**) Cumulative effects of immune cell infiltration with survival of HCC patient using TIMER; (**b**) The immune infiltrate analysis between HOXB4 expression and HCC in the TIMER dataset; (**c**) The correlation between HOXB4 and CD8a expression in HCC using GEPIA; (**d**) Efficacy of HOXB4 knockdown and overexpression in Hepa1-6 cells; (**e**) Representative immunoblots of PD-L1 in Hepa1-6 cells with HOXB4 knockdown and overexpression; (**f**-**g**) Tumor volume and growth curves of subcutaneous transplanted tumor of C57BL/6 mice injected with Hepa1-6 cells, $N=6$; (**h**) Representative hematoxylin and eosin staining images of tumor tissues. Scale bars, 100 μm; (**i**) Representative immunoblots of HOXB4 and PD-L1 in tumor tissues of C57BL/6 mice injected with indicated Hepa1-6 cells, $N=3$; (**j**) Immunohistochemical staining and quantitative data of CD3 in tumor tissues of C57BL/6 mice injected with indicated Hepa1-6 cells, $N=6$. Scale bars, 50 μm; (**k**) The percentage of CD8 + and CD4 + T cells in tumor tissues of C57BL/6 mice injected with indicated Hepa1-6 cells using flow cytometry assay, $N=6$. Data are expressed as mean ± SD. $^{**}p<0.01$, $^{***}p<0.001$ vs. EV^{Tet}+dox; $^{\#}p<0.05$, $^{\#\#}p<0.01$, $^{\#\#\#}p<0.001$ vs. $shNC^{Tet}$+dox

downstream targets of METTL7B in HCC, RNA-seq data available for METTL7B knockdown revealed that TKT was significantly downregulated upon METTL7B knockdown (Fig. 7a). TKT mRNA levels was also positively regulated by METTL7B in Li-7 cells (Fig. 7b). It has been confirmed that activated TKT increased PD-L1 expression, leading to immune evasion and HCC metastasis [24]. According to the results of PCR and WB, TKT expression was upregulated in HCC cell lines (Fig. 7b). HOXB4 knockdown increased TKT expression, while METTL7B downregulated abolished HOXB4 effects (Fig. 7d). Therefore, TKT might be the downstream of HOXB4/METTL7B axis. The presence of high m6A sites in TKT mRNA was found using Sramp dataset (Fig. 7c). METTL7B overexpression showed to cause a significantly higher increase in TKT mRNA enrichment compared to IgG using m6A-IP-qPCR assay (Fig. 7d). siRNA targeting TKT was designed to investigate whether METTL7B plays a role through regulating TKT in HCC cells (Fig. 7e and f). TKT silencing could suppress the promoting effects of METTL7B overexpression on HCC cell proliferation, metastasis, and PD-L1 expression (Fig. 7g and i). The same results were verified with the administration of TKT inhibitor (N3PT) (Fig. S5). Collectively, above findings indicated that METTL7B overexpression promoted malignant phenotypes of HCC by increasing TKT mRNA expression via m6A modification.

Discussion

It is essential to investigate the underlying molecular complexity of HCC to overcome the poor prognosis. m6A modification has been found to be altered and resulted oncogenic potential in various cancer [18]. The present study demonstrated that HOXB4 was downregulated in HCC. HOXB4 overexpression inhibiting malignant phenotypes and immune evasion both in vivo and in vitro. We further identified the HOXB4-METTL7B negative regulation loop based on the results of RNA-seq, and verified METTL7B promoted malignant phenotypes and immune evasion in vitro. The dataset analysis and m6A-IP-qPCR supported that METTL7B increase TKT mRNA expression by increasing m6A modification. Overall, our findings revealed that HOXB4 negatively regulated METTL7B/TKT axis, which, in turn, inhibits malignant phenotypes in HCC.

The HOX genes are an evolutionarily conserved family of transcription factors. HOX gene downregulated expression has been observed in malignancies, influencing tumorigenesis [37]. Previous study reported that the expression of HOXB4 was low in many tumor [10, 38]. In cervical cancer, the downregulation of HOXB4 stimulated the proliferation of tumor cells [10]. The related reports of HOXB4 in HCC was lack. In our study, we revealed the anti-tumors effects of HOXB4 overexpression by inhibiting tumor growth and promoting tumor cell apoptosis.

EMT affects the malignant progression of tumors, resulting in cancer metastasis by facilitating tumor cell invasion [39]. E-cadherin was a transmembrane glycoprotein that closely related to intercellular adhesion and served a typical epithelial cell marker. Vimentin and N-cadherin were considered important markers for mesenchymal cells [40]. During tumor metastasis, epithelial cells would lose adhesion and acquire invasive ability, making EMT essential for HCC malignant progression [41]. In the study of Li et al. [38]. HOXB4 could affect malignant progression of ovarian cancer cell via the regulation of E-cadherin expression and Vimentin expression. The enforced expression of HOXB4 suppressed breast cancer cell migration via inhibiting EMT [11]. In our study, we observed that HOXB4 might suppressed the EMT, thereby inhibiting HCC cell migration and invasion.

The increase immune cell infiltration was correlated with better outcomes in HCC patients [42]. HOXB4 expression in colorectal cancer tissues could influence immune infiltration [9]. PD-L1 upregulation facilitated cancer progression through immune surveillance evasion and T cell exhaustion [43]. The promotion of PD-L1 would lead to the inhibition of CD8 + T cell in HCC [44]. In bone marrow progenitor cells, HOXB4 could regulate PD-L1 expression and T cell function [15]. In our study, we found that HOXB4 overexpression inhibited the immune evasion in HCC by increasing T cell infiltration and inhibiting PD-L1 expression. Above all, we revealed that HOXB4 inhibited the malignant phenotypes and immunosuppression in HCC.

m6A modification played a role in HCC immunoregulation and ontogenesis [45, 46]. The methyltransferase family genes were involved in m6A modification and

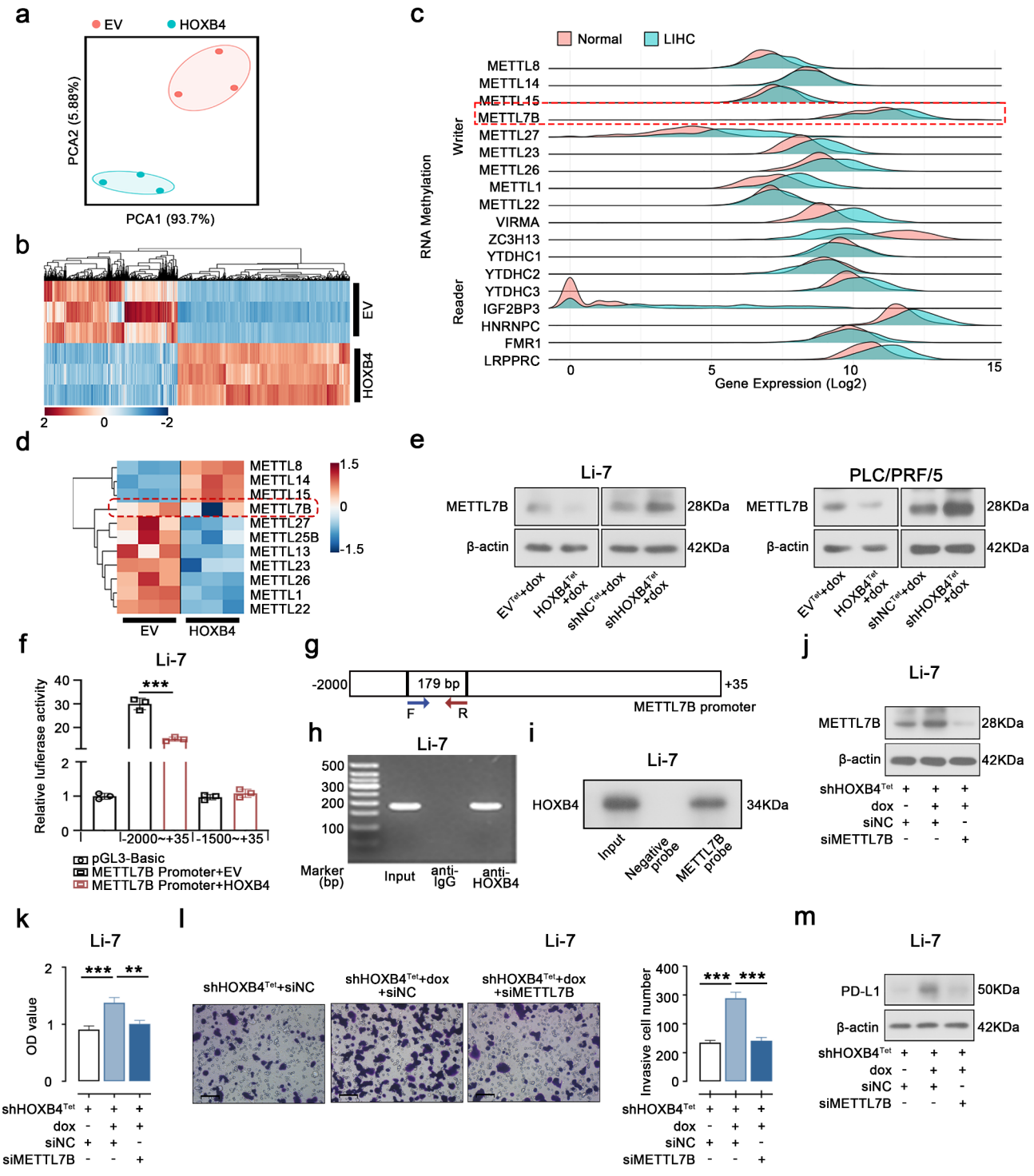

Fig. 6 METTL7B is a target gene of HOXB4 and functions in hepatocellular carcinoma. (**a**) Principal component analysis (PCA) of HOXB4-overexpressed Li-7 cells and its control cells; (**b**) Heatmap showing DEGs in HOXB4-overexpressed Li-7 cells.|Log2FC| > 1 and adj. $p < 0.005$ were cutoff values; (**c**) The gene expression levels of m6A regulators in HCC using TNMplot; (**d**) Heatmap showing expression of methyltransferase-like proteins in HOXB4-overexpressed Li-7 cells; (**e**) Representative immunoblots of METTL7B protein in HCC cells with upregulated or downregulated HOXB4 expression; (**f**) Dual-luciferase assay determine the binding of HOXB4 to METTL7B promoter regions in HCC; (**g**) Schematic of the METTL7B gene showing sequence locations of ChIP primer pairs; (**h**) ChIP results of HOXB4 binding to the promoter region of METTL7B; (**i**) The binding of HOXB4 and METTL7B was performed using Pull-down assay; (**j**) Representative immunoblots of METTL7B in Li-7 cells with METTL7B and HOXB4 knockdown; (**k**) Cell viability of Li-7 cells with METTL7B and HOXB4 knockdown; (**l**) The invasion ability of Li-7 cells with METTL7B and HOXB4 knockdown. Scale bar, 100 μm. (**m**) Representative immunoblots of PD-L1 in Li-7 cells with METTL7B and HOXB4 knockdown. Data are expressed as mean ± SD, $N = 3$. $^{**}p < 0.01$, $^{***}p < 0.001$

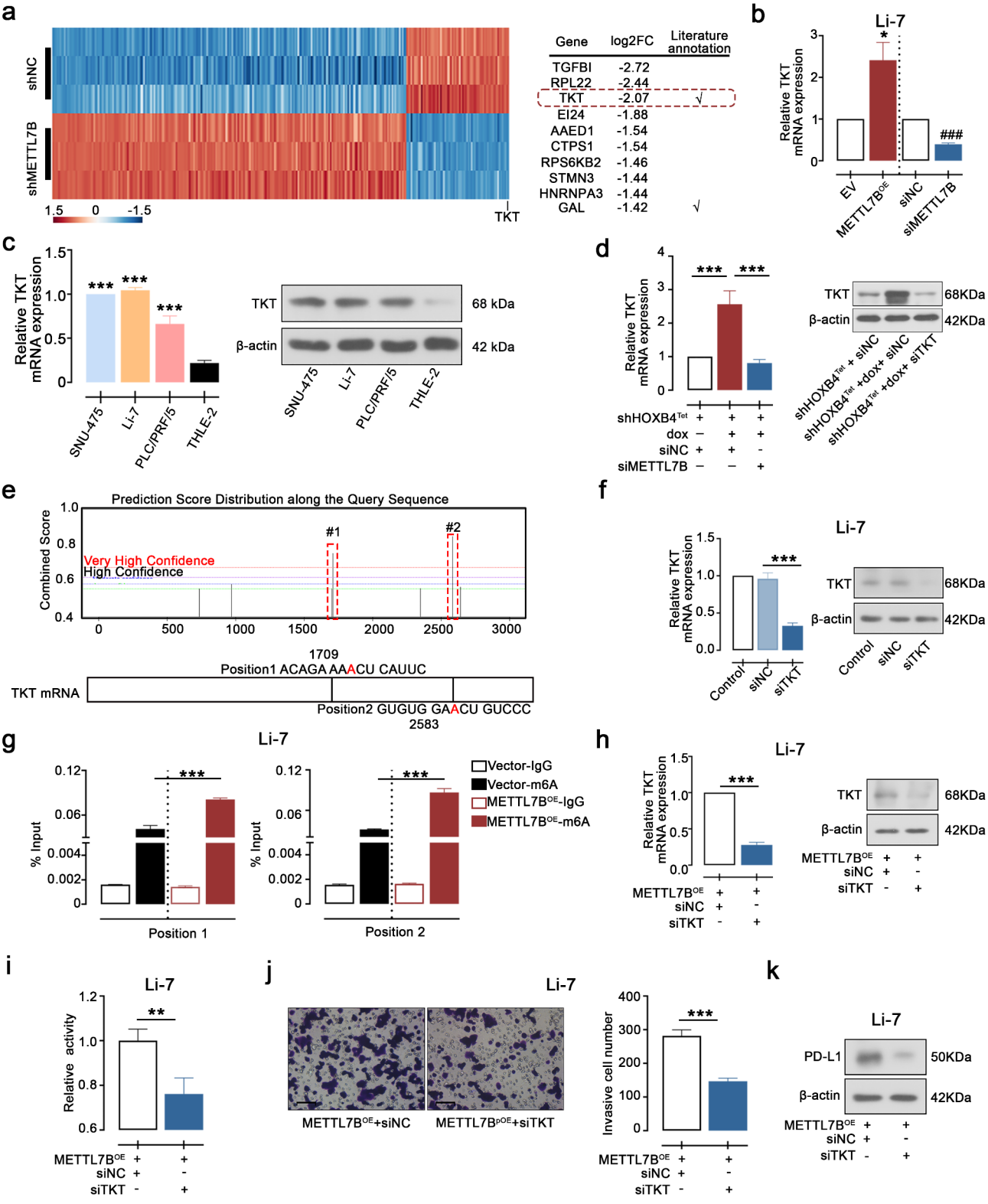

Fig. 7 (See legend on next page.)

(See figure on previous page.)

Fig. 7 METTL7B exerts its role in hepatocellular carcinoma via m6A-dependent promotion of TKT. (**a**) The heatmap of differential expression genes (DEGs) of shMETTL7B cells. Data was obtained from GEO with dataset accession number GSE142278.|Log2FC| > 1 and adj. $p < 0.005$ were cutoff values (left panel). Table of top 10 genes significantly reduced in shMETTL7B cells (right panel). (**b**) TKT mRNA levels in Li-7 cells with METTL7B knockdown or overexpression. (**c**) TKT mRNA and protein expression and in SNU-475, Li-7, PLC/PRF/5 and normal THLE-2 cells. (**d**) TKT mRNA and protein levels in HOXB4 knockdown Li-7 cells transfected with siMETTL7B. (**e**) The predicted m6A motifs in the coding sequence (CDS) of TKT with high confidence using SRAMP. (**f**) The m6A level in METTL7B overexpressed Li-7 cells after m6A immunoprecipitation. (**g**) Efficacy of TKT knockdown in Li-7 cells; (**h**) TKT mRNA and protein levels in METTL7B-overexpressed Li-7 cells with TKT knockdown; (**i**) Cell viability of METTL7B-overexpressed Li-7 cells with TKT knockdown; (**j**) The invasion ability of METTL7B-overexpressed Li-7 cells with TKT knockdown. Scale bar, 100 μm; (**k**) Representative immunoblots of PD-L1 in METTL7B-overexpressed Li-7 cells with TKT knockdown. Data are expressed as mean ± SD, $N = 3$. (**b**) $^{*}p < 0.05$ vs. EV; $^{\#\#\#}p < 0.001$ vs. siNC, (**c**-**k**) $^{*}p < 0.05$, $^{**}p < 0.01$, $^{***}p < 0.001$

participated in the progression of HCC [20, 45]. In the present study, METTL7B expression was significantly downregulated in HOXB4-overexpressed cells. Combining with the expression of methyltransferase family genes in HCC tissues, we proposed that METTL7B might serve as the downstream of HOXB4 in HCC. In vitro cell experiments revealed that the downregulation of METTL7B in acute lymphoblastic leukemia reduced cell proliferation [47]. Overexpression of METTL7B could promote the malignant phenotypes in glioma [48]. METTL7B was presented at elevated levels in HCC and correlated with PD-L1 expression [34, 49], but its role in HCC remined unknown. Hence in, we first verified the promotion of METTL7B in malignant phenotypes of HCC cells. Based on previous literature reports, HOXB4 might act as a transcriptional activator and repressor [50–52]. HOXB4 transcriptionally inhibited downstream target gene expression in cervical cancer [10] and ovarian cancer [53]. Our results demonstrated that HOXB4 transcriptionally inhibited METTL7B expression by binding to the promoter region of METTL7B. The elevated capability of proliferation, metastasis, and immune escape, induced by HOXB4 knockdown, were reversed in METTL7B-depleted Li-7 cells. The above results suggested that HOXB4 might exert its function in HCC through inhibiting METTL7B expression.

During carcinogenesis, methyltransferases generally functioned by regulating the expression of their mRNA targets through m6A modifications [54]. We further investigated the target genes of METTL7B, and found that TKT expression was significantly decreased in METTL7B-depleted cells. TKT is an enzyme that presented in most tumor tissues [55]. Recent research verified that TKT promoted HCC cell proliferation and migration [22]. Previous study has demonstrated that activated TKT led to immune escape and HCC cell metastasis by increasing PD-L1 expression [24]. As an m6A modification writer, we confirmed that METTL7B overexpression promoted TKT expression via m6A modification. With the administration of siTKT and N3PT (TKT inhibitor), we demonstrated that downregulated TKT reversed the effects of METTL7B overexpression on HCC malignant phenotypes. Taken together, TKT was involved in METTL7B-mediated the promotion of immune evasion and the proliferative and metastatic capability of HCC cells.

In conclusion, we reveal for the first time that HOXB4 displays anti-tumor effects through suppresses the malignant phenotype and immune evasion in HCC. HOXB4 transcriptionally suppressed METTL7B expression. HOXB4/METTL7B axis functioned in HCC by regulating TKT expression in the m6A-dependent manner. Collectively, our results suggest that the increased HOXB4 expression might be a potential strategy to alleviate HCC progression.

Abbreviations

HCC	Hepatocellular carcinoma
HOXB4	Homeobox B4
METTL7B	Methyltransferase-like 7B
m6A	N6-methyladenosine
TKT	Transketolase
RNA-seq	RNA-sequencing
MTT	Methyl Thiazolyl

Supplementary Information

The online version contains supplementary material available at https://doi.org/10.1186/s13062-025-00620-3.

Supplementary Material 1

Supplementary Material 2

Supplementary Material 3

Supplementary Material 4

Supplementary Material 5

Acknowledgements

Not applicable.

Author contributions

ES. G planned experiments, analyzed data, contributed reagents and essential material, and wrote the paper. L. L performed experiments, analyzed data, and wrote the paper. JK. Y performed experiments, analyzed data. YJ. Z wrote the paper and performed experiments. L. B analyzed data and contributed reagents and essential material. WW. Z performed experiments. QY. H analyzed data. HF. W performed experiments. HQ. L analyzed data. All authors read and approved the final manuscript.

Funding

Our research was supported by Natural Science Foundation of Henan Province (212300410266) and the Joint Construction Project of Henan Medical Science and Technology Tackling Plan (2018020101).

Data availability

The data that support the findings of this study are available from the corresponding author, upon reasonable request.

Declarations

Ethics approval and consent to participate

All animal experiments were conducted in accordance with the ethical standards of animal care and approved by the Life Science Ethics Review Committee of Zhengzhou University (March 18, 2022).

Consent for publication

Not applicable.

Competing interests

The authors declare no competing interests.

Author details

[1]Department of Infectious Diseases, The First Affiliated Hospital of Zhengzhou University, Zhengzhou 450052, China
[2]Precision Medicine Center, Gene Hospital of Henan Province, The First Affiliated Hospital of Zhengzhou University, Zhengzhou 450052, China
[3]Department of Osteology, Yellow River Central Hospital of the Yellow River Conservancy Commission, Zhengzhou 450003, China
[4]Experimental Medicine Center, Tongji Hospital, Tongji Medical College, Huazhong University of Science and Technology, Wuhan 430030, China
[5]Department of Emergency, Henan Province Hospital of Traditional Chinese Medicine, Zhengzhou 450002, China

Received: 25 July 2024 / Accepted: 17 February 2025
Published online: 05 March 2025

References

1. Forner A, Reig M, Bruix J. Hepatocellular carcinoma. Lancet. 2018;391:1301–14. https://doi.org/10.1016/S0140-6736(18)30010-2.
2. Heimbach JK, et al. AASLD guidelines for the treatment of hepatocellular carcinoma. Hepatology. 2018;67:358–80. https://doi.org/10.1002/hep.29086.
3. Khemlina G, Ikeda S, Kurzrock R. The biology of hepatocellular carcinoma: implications for genomic and immune therapies. Mol Cancer. 2017;16:149. https://doi.org/10.1186/s12943-017-0712-x.
4. Novikova MV, Khromova NV, Kopnin PB. Components of the hepatocellular carcinoma microenvironment and their role in tumor progression. Biochem (Mosc). 2017;82:861–73. https://doi.org/10.1134/S0006297917080016.
5. Yang C, Huang X, Liu Z, Qin W, Wang C. Metabolism-associated molecular classification of hepatocellular carcinoma. Mol Oncol. 2020;14:896–913. https://doi.org/10.1002/1878-0261.12639.
6. Jin Z, et al. Comprehensive analysis of HOX family members as novel diagnostic and prognostic markers for hepatocellular carcinoma. J Oncol. 2022;2022(5758601). https://doi.org/10.1155/2022/5758601.
7. Wang L, et al. HOXD3 was negatively regulated by YY1 recruiting HDAC1 to suppress progression of hepatocellular carcinoma cells via ITGA2 pathway. Cell Prolif. 2020;53:e12835. https://doi.org/10.1111/cpr.12835.
8. Dang Y, et al. Interleukin 1beta-mediated HOXC10 overexpression promotes hepatocellular carcinoma metastasis by upregulating PDPK1 and VASP. Theranostics. 2020;10:3833–48. https://doi.org/10.7150/thno.41712.
9. Wang L, et al. HOXB4 Mis-Regulation induced by Microcystin-LR and correlated with immune infiltration is unfavorable to colorectal Cancer prognosis. Front Oncol. 2022;12:803493. https://doi.org/10.3389/fonc.2022.803493.
10. Lei D, Yang WT, Zheng PS. HOXB4 inhibits the proliferation and tumorigenesis of cervical cancer cells by downregulating the activity of Wnt/beta-catenin signaling pathway. Cell Death Dis. 2021;12:105. https://doi.org/10.1038/s41419-021-03411-6.
11. Zhou G, Liu X, Xiong B, Sun Y. Homeobox B4 inhibits breast cancer cell migration by directly binding to StAR-related lipid transfer domain protein 13. Oncol Lett. 2017;14:4625–32. https://doi.org/10.3892/ol.2017.6825.
12. Bonfim-Silva R, et al. Functional analysis of HOXA10 and HOXB4 in human Medulloblastoma cell lines. Int J Oncol. 2017;51:1929–40. https://doi.org/10.3892/ijo.2017.4151.
13. Bradley CA, Immunotherapy. CD8(+) T cells - burn fat, get fit. Nat Rev Cancer. 2017;17:635. https://doi.org/10.1038/nrc.2017.94.
14. Li Q, et al. PRDM1/BLIMP1 induces cancer immune evasion by modulating the USP22-SPI1-PD-L1 axis in hepatocellular carcinoma cells. Nat Commun. 2022;13:7677. https://doi.org/10.1038/s41467-022-35469-x.
15. Schroder M, et al. Identification of inhibitors of myeloid-derived suppressor cells activity through phenotypic chemical screening. Oncoimmunology. 2017;6:e1258503. https://doi.org/10.1080/2162402X.2016.1258503.
16. El-Serag HB, Marrero JA, Rudolph L, Reddy KR. Diagnosis and treatment of hepatocellular carcinoma. Gastroenterology. 2008;134:1752–63. https://doi.org/10.1053/j.gastro.2008.02.090.
17. Jiang X, et al. The role of m6A modification in the biological functions and diseases. Signal Transduct Target Ther. 2021;6:74. https://doi.org/10.1038/s41392-020-00450-x.
18. Sun T, Wu R, Ming L. The role of m6A RNA methylation in cancer. Biomed Pharmacother. 2019;112:108613. https://doi.org/10.1016/j.biopha.2019.108613.
19. Chen M, et al. RNA N6-methyladenosine methyltransferase-like 3 promotes liver cancer progression through YTHDF2-dependent posttranscriptional Silencing of SOCS2. Hepatology. 2018;67:2254–70. https://doi.org/10.1002/hep.29683.
20. Li TH, et al. Identification METTL18 as a potential prognosis biomarker and associated with immune infiltrates in hepatocellular carcinoma. Front Oncol. 2021;11:665192. https://doi.org/10.3389/fonc.2021.665192.
21. Ma JZ, et al. METTL14 suppresses the metastatic potential of hepatocellular carcinoma by modulating N(6) -methyladenosine-dependent primary MicroRNA processing. Hepatology. 2017;65:529–43. https://doi.org/10.1002/hep.28885.
22. Qin Z, et al. Transketolase (TKT) activity and nuclear localization promote hepatocellular carcinoma in a metabolic and a non-metabolic manner. J Exp Clin Cancer Res. 2019;38:154. https://doi.org/10.1186/s13046-019-1131-1.
23. Jia D, et al. Novel transketolase inhibitor oroxylin A suppresses the non-oxidative Pentose phosphate pathway and hepatocellular carcinoma tumour growth in mice and patient-derived organoids. Clin Transl Med. 2022;12:e1095. https://doi.org/10.1002/ctm2.1095.
24. Zhang J, et al. Elevated FBXL6 expression in hepatocytes activates VRK2-transketolase-ROS-mTOR-mediated immune evasion and liver cancer metastasis in mice. Exp Mol Med. 2023;55:2162–76. https://doi.org/10.1038/s12276-023-01060-7.
25. Ashrafizadeh M, et al. New insight towards development of Paclitaxel and docetaxel resistance in cancer cells: EMT as a novel molecular mechanism and therapeutic possibilities. Biomed Pharmacother. 2021;141:111824. https://doi.org/10.1016/j.biopha.2021.111824.
26. Ishii Y, Nakasato Y, Kobayashi S, Yamazaki Y, Aoki T. A study on angiogenesis-related matrix metalloproteinase networks in primary hepatocellular carcinoma. J Exp Clin Cancer Res. 2003;22:461–70.
27. Li Q, Han J, Yang Y, Chen Y. PD-1/PD-L1 checkpoint inhibitors in advanced hepatocellular carcinoma immunotherapy. Front Immunol. 2022;13:1070961. https://doi.org/10.3389/fimmu.2022.1070961.
28. Brown ZJ, Ruff SM, Pawlik TM. The effect of liver disease on hepatic microenvironment and implications for immune therapy. Front Pharmacol. 2023;14:1225821. https://doi.org/10.3389/fphar.2023.1225821.
29. Paco A, de Bessa Garcia A S, Freitas R. Methylation in HOX clusters and its applications in Cancer therapy. Cells. 2020;9. https://doi.org/10.3390/cells9071613.
30. Chen Y, et al. WTAP facilitates progression of hepatocellular carcinoma via m6A-HuR-dependent epigenetic Silencing of ETS1. Mol Cancer. 2019;18:127. https://doi.org/10.1186/s12943-019-1053-8.
31. Shi H, Wei J, He C, Where. When, and how: Context-Dependent functions of RNA methylation writers, readers, and erasers. Mol Cell. 2019;74:640–50. https://doi.org/10.1016/j.molcel.2019.04.025.
32. Dai YZ, et al. METTL16 promotes hepatocellular carcinoma progression through downregulating RAB11B-AS1 in an m(6)A-dependent manner. Cell Mol Biol Lett. 2022;27. https://doi.org/10.1186/s11658-022-00342-8.
33. Lei Y, et al. Protein arginine methyltransferase 3 promotes Glycolysis and hepatocellular carcinoma growth by enhancing arginine methylation of lactate dehydrogenase A. Clin Transl Med. 2022;12:e686. https://doi.org/10.1002/ctm2.686.
34. Luo C, et al. A whole exon Screening-Based score model predicts prognosis and immune checkpoint inhibitor therapy effects in Low-Grade glioma. Front Immunol. 2022;13:909189. https://doi.org/10.3389/fimmu.2022.909189.
35. Ye D, et al. METTL7B promotes migration and invasion in thyroid cancer through epithelial-mesenchymal transition. J Mol Endocrinol. 2019;63:51–61. https://doi.org/10.1530/JME-18-0261.
36. Liu D, et al. METTL7B is required for Cancer cell proliferation and tumorigenesis in Non-Small cell lung Cancer. Front Pharmacol. 2020;11:178. https://doi.org/10.3389/fphar.2020.00178.

37. Yadav C, et al. Role of HOX genes in cancer progression and their therapeutical aspects. Gene. 2024;919:148501. https://doi.org/10.1016/j.gene.2024.148501.
38. Li N, Gou JH, Xiong J, You JJ, Li ZY. HOXB4 promotes the malignant progression of ovarian cancer via DHDDS. BMC Cancer. 2020;20:222. https://doi.org/10.1186/s12885-020-06725-4.
39. Heerboth S, et al. EMT and tumor metastasis. Clin Transl Med. 2015;4:6. https://doi.org/10.1186/s40169-015-0048-3.
40. Lamouille S, Xu J, Derynck R. Molecular mechanisms of epithelial-mesenchymal transition. Nat Rev Mol Cell Biol. 2014;15:178–96. https://doi.org/10.1038/nrm3758.
41. Wu J, et al. HMGA2 overexpression-induced ovarian surface epithelial transformation is mediated through regulation of EMT genes. Cancer Res. 2011;71:349–59. https://doi.org/10.1158/0008-5472.CAN-10-2550.
42. Cai X, et al. CDK4/6 Inhibition enhances T-cell immunotherapy on hepatocellular carcinoma cells by rejuvenating immunogenicity. Cancer Cell Int. 2024;24:215. https://doi.org/10.1186/s12935-024-03351-z.
43. Wang Q, et al. FAT10 induces immune suppression by upregulating PD-L1 expression in hepatocellular carcinoma. Apoptosis. 2024. https://doi.org/10.1007/s10495-024-01982-1.
44. Chen J, et al. GOLM1 exacerbates CD8(+) T cell suppression in hepatocellular carcinoma by promoting Exosomal PD-L1 transport into tumor-associated macrophages. Signal Transduct Target Ther. 2021;6:397. https://doi.org/10.1038/s41392-021-00784-0.
45. Yang L, et al. N6-methyladenosine RNA methylation in liver diseases: from mechanism to treatment. J Gastroenterol. 2023;58:718–33. https://doi.org/10.1007/s00535-023-02008-4.
46. Pan XY, Huang C, Li J. The emerging roles of m(6)A modification in liver carcinogenesis. Int J Biol Sci. 2021;17:271–84. https://doi.org/10.7150/ijbs.50003.
47. Zhang L, Liu X, Zhou S, Wang P, Zhang X. Glycolysis modulation by METTL7B shapes acute lymphoblastic leukemia cell proliferation and chemotherapy response. Hum Cell. 2024;37:478–90. https://doi.org/10.1007/s13577-024-01025-6.
48. Li Z, Song Y, Zhang J. LncRNA PDCD4-AS1 promotes the progression of glioma by regulating miR-30b-3p/METTL7B signaling. Oxid Med Cell Longev. 2023;2023(3492480). https://doi.org/10.1155/2023/3492480.
49. Philipp TM, Scheller AS, Krafczyk N, Klotz LO, Steinbrenner H. Methanethiol: A scent mark of dysregulated sulfur metabolism in Cancer. Antioxid (Basel). 2023;12. https://doi.org/10.3390/antiox12091780.
50. Beslu N, et al. Molecular interactions involved in HOXB4-induced activation of HSC self-renewal. Blood. 2004;104:2307–14. https://doi.org/10.1182/blood-2004-04-1653.
51. Oshima M, et al. Genome-wide analysis of target genes regulated by HoxB4 in hematopoietic stem and progenitor cells developing from embryonic stem cells. Blood. 2011;117:e142–150. https://doi.org/10.1182/blood-2010-12-323212.
52. Schiedlmeier B, et al. HOXB4's road map to stem cell expansion. Proc Natl Acad Sci U S A. 2007;104:16952–7. https://doi.org/10.1073/pnas.0703082104.
53. Liu J, et al. LINC00629, a HOXB4-downregulated long noncoding RNA, inhibits Glycolysis and ovarian cancer progression by destabilizing c-Myc. Cancer Sci. 2024;115:804–19. https://doi.org/10.1111/cas.16049.
54. Macatee RJ, et al. Psychometric properties of the late positive potential in combat-exposed veterans. Int J Psychophysiol. 2021;161:13–26. https://doi.org/10.1016/j.ijpsycho.2021.01.001.
55. Hao S, et al. The role of transketolase in human cancer progression and therapy. Biomed Pharmacother. 2022;154:113607. https://doi.org/10.1016/j.biopha.2022.113607.

Publisher's note